PROCEEDINGS, Thirty-Fourth Workshop on Geothermal Reservoir Engineering
Stanford University, Stanford, California, February 9-11, 2009
SGP-TR-187

TIME-DEPENDENT SEISMIC TOMOGRAPHY OF GEOTHERMAL SYSTEMS

Bruce R. Julian[1], Gillian R. Foulger[2]

[1]U.S. Geological Survey, 345 Middlefield Rd., Menlo Park, CA 94306
e-mail: julian@usgs.gov

[2]Dept. Earth Sciences, University of Durham, Science Laboratories, South Rd., Durham, DH1 3LE, U.K.
e-mail: g.r.foulger@durham.ac.uk

ABSTRACT

Temporal changes in seismic wave speeds in the Earth's crust have been measured at several geothermal areas, notably The Geysers in California, in studies that used three-dimensional seismic tomography. These studies used conventional tomography methods to invert seismic-wave arrival time data sets for different epochs independently and assumed that any differences in the derived structures reflect real temporal variations. Such an assumption is dangerous because the results of repeated tomography experiments would differ even if the structure did not change, simply because of variation in the seismic ray distribution caused by the natural variation in earthquake locations. This problem can be severe when changes in the seismicity distribution are systematic, as, for example, when many data come from earthquake swarms. The sudden change in the ray distribution can produce artifacts that mimic changes in the seismic wave speeds at the time of a swarm. Even if the source locations did not change (if only explosion data were used, for example), derived structures would inevitably differ because of observational errors.

In order to determine what changes are real and what are artifacts, we have developed a new tomography method, *tomo4d*, that inverts multiple data sets simultaneously, imposing constraints to minimize the differences between the models for different epochs. This problem is similar to that of seeking models similar to some *a priori* initial assumption, and a method similar to "damped least squares" can solve it. We present an algorithm for performing this computation efficiently. Using our program, inverting multiple epochs simultaneously is comparable in difficulty to inverting them independently. We illustrate the program's performance using synthetic arrival times.

INTRODUCTION

A variety of physical processes can cause the seismic-wave speeds in geothermal and hydrocarbon reservoirs to vary with time. These include changes in the stiffness of the rock matrix caused by drying or wetting of clay minerals (Boitnott & Boyd, 1996) and changes in pore-fluid compressibility caused by CO_2 flooding (Wang *et al.*, 1998; Daley *et al.*, 2007) or fluid extraction (Gunasekera *et al.*, 2003). Figure 1 shows the particularly strong changes that occurred in The Geysers geothermal reservoir, California, in the 1990s. Measuring such variations has many important applications, *e.g.*, monitoring of reservoir exploitation and of underground CO_2 sequestration.

METHOD

Tomographic investigations of temporal changes in Earth structure have until now been conducted by inverting seismic-wave arrival time data sets for different epochs independently, assuming that differences in the resulting models arise from real temporal variations. This assumption is questionable, however, because the results of repeated tomography experiments would differ even if the structure did not change, because of variations in the seismic ray distributions caused by natural variation in earthquake locations. Even if the source locations did not change (if explosion data were used, for example) and the seismometer distribution were held fixed, differences in the derived models would be expected because of random observational errors. The reality of the temporal changes at The Geysers mentioned above is not subject to serious doubt, because of their magnitude and their association with a large pore-pressure drop in the geothermal reservoir, but some weaker reported changes remain open to question. Among these are possible changes between 1989 and 1997 in the ratio of the elastic-wave speeds, V_P/V_S, associated with CO_2 emissions at Mammoth Mountain in Long Valley caldera, California (Foulger *et al.*, 2003) and possible recent changes at the Coso geothermal area, California (Julian *et al.*, 2008).

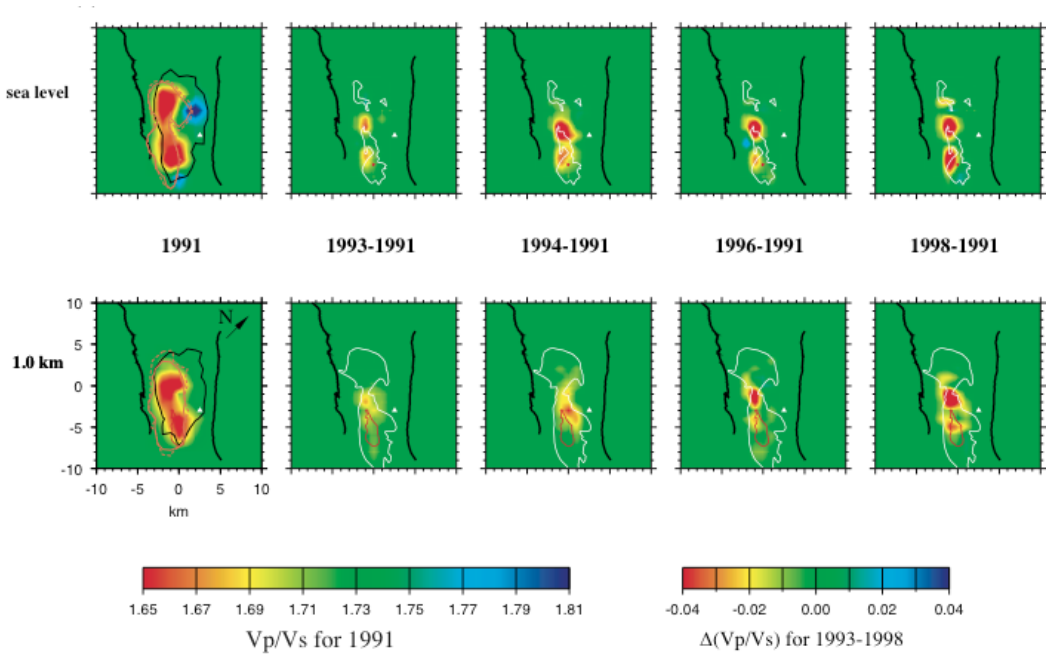

Fig. 1: *Maps showing changes in the V_P/V_S ratio at two depths at The Geysers geothermal area, California, between 1991 and 1998, as determined by Gunasekera et al. (2003) by inverting five data sets independently.*

Some studies, such as that of Foulger *et al.* (2003) of Long Valley caldera, have attempted to deal with this sampling problem by performing a series of inversions, alternating between two epochs and using the model derived in one inversion as the starting model in the next inversion of data from the other epoch, but this procedure is awkward and time-consuming, has no rigorous basis, and furthermore offers no help in assessing the effects of random observational errors.

An alternative approach, which makes it possible to determine what changes are truly required by the data, is to invert multiple data sets simultaneously, minimizing the difference between the models for different epochs as well as the difference between observed and predicted arrival times. This problem is similar to that of seeking models consistent with an *a priori* assumed model, and it can be solved using a technique similar to the "damped least squares" method (Marquardt, 1963). Solving for two epochs simultaneously requires the determination of twice as many parameters as solving for a single epoch does, and the most straightforward solution method requires eight times the computational labor, and thus quadruples the labor compared to solving for two epochs independently. In most cases the system of normal equations for the two-epoch problem is sparse, however, and we have derived an algorithm, *tomo4d*, that takes advantage of this fact to solve the equations with only slightly more labor than is needed to solve for each epoch independently.

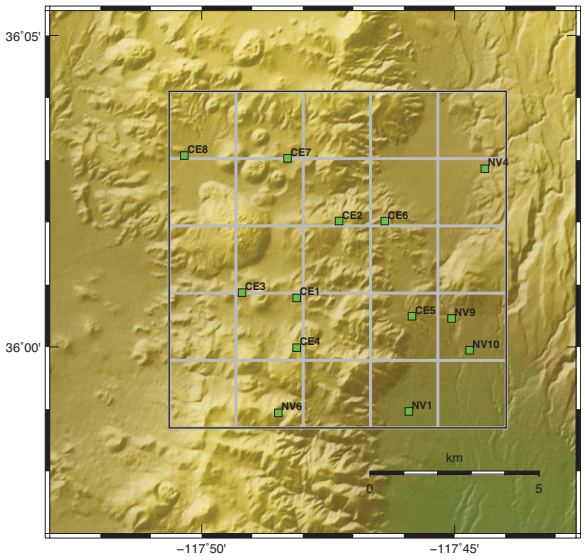

Fig. 2: *Map of the Coso geothermal area, eastern California, used as the basis for synthetic tests. Green squares: Stations of the U. S. Navy's telemetered seismometer network. The tomographic grid has nodes spaced by 2 km horizontally and 1 km vertically.*

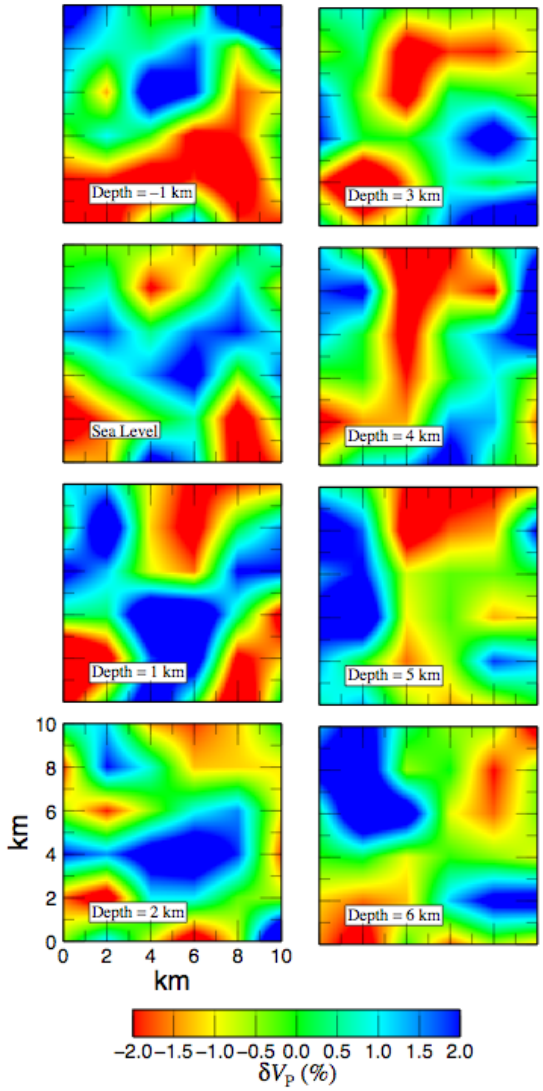

Fig. 3: *Maps of the compressional wave-speed V_P at different depths in the random time-independent model used in synthetic tests. The deterministic component of V_P is purely depth-dependent. The random component has a Gaussian covariance with a standard deviation of 0.1 km s^{-1} and correlation distances of 2 km horizontally and 1 km vertically. The grid geometry is shown in Figure 2. Percent deviations from the mean at each depth are shown.*

TESTS WITH SYNTHETIC DATA

To illustrate this method, we compute theoretical arrival-time data sets for pseudo-random local Earth models and hypocenter locations and an actual seismometer distribution, and invert these data sets both independently and using *tomo4d*. We perform this exercise using both time-independent and temporally varying Earth models and different sets of assumed earthquake locations, which give both dense and sparse distributions of rays and both random and systematic differences in their sampling of the structure with time. In all cases we use a real (non-random) distribution of seismometers, the innermost 13 stations of the U.S. Navy's permanent network at the Coso geothermal area, California (Figure 2).

Apparent Temporal Variations Caused by Changes in Ray Distribution

Because of natural changes in the locations of earthquakes, repeated tomographic inversions would be expected to give different results even if the wave speeds in the Earth did not vary with time. To simulate this phenomenon, we invert theoretical *P*-wave arrival-time data sets generated by tracing rays through the pseudo-random model shown in Figure 3. We investigate two types of situation: Statistically uniform spatial distributions of earthquakes, such as might represent natural background seismicity, and strongly clustered earthquakes, such as might occur in an earthquake swarm or aftershock sequence.

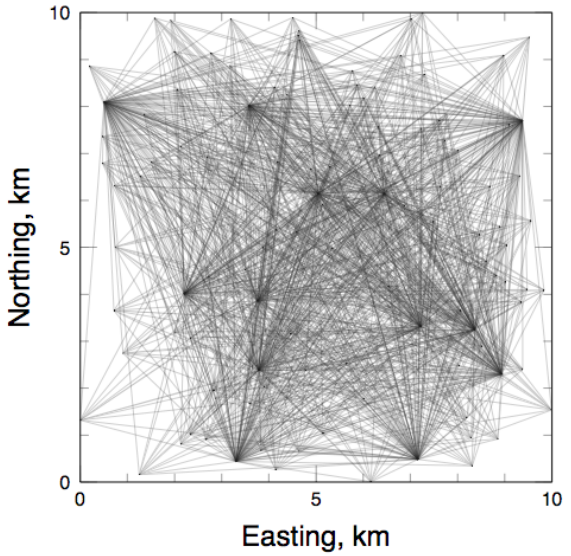

Fig. 4: *Surface projections of ray paths (represented as straight lines) for a sparse pseudo-random theoretical arrival-time data set intended to represent spatially uniform background seismicity. Rays connect each of 100 pseudo-random hypocenter locations with the 13 seismometer locations shown in Figure 2. The earthquake hypocenter locations have a uniform probability distribution over the 10 km × 10 km × 10 km volume.*

In order to reduce potentially complicating effects, we made several simplifications of reality. We inverted exact theoretical arrival times, without attempting to simulate observational errors, and we

did not attempt to solve for hypocenter locations, but instead used the true locations as inputs to the inversion process. In reality, observational errors and uncertainty about hypocentral locations would complicate the task of identifying artifacts such as spurious temporal variations in wave speeds. We inverted theoretical arrival times for seismic *P* phases only, and thus solved for only the compressional-wave speed V_P . In reality, the shear-wave speed V_S is of great intrinsic interest, and *S*-phase times are particularly valuable for constraining hypocentral locations. To minimize nonlinear effects, we used a pseudo-random model (Figure 3) with comparatively weak lateral variations in wave speed (about 2%) and performed only a single tomographic iteration. This restriction, combined with the use of step-size damping, means that our derived models resolve only the strongest of the pseudo-random variations.

Random Variations in Ray Distribution

Figure 4 shows an example of ray paths for a sparse, statistically uniform distribution of random hypocenter locations intended to represent un-clustered background seismicity. We inverted pairs of theoretical data sets computed for such random rays using two approaches: independent inversions and joint inversions using *tomo4d* to suppress differences between derived models that are not actually required by the data.

Figure 5 shows the results of inverting a pair of data sets independently, and Figure 6 shows the results from *tomo4d*. All these results exhibit several large-scale anomalies, most of which correspond to features in the pseudo-random model used to generate the theoretical data (Figure 3), although the inevitable under-sampling of the structure by rays causes many other features of the models not to be imaged well. The results for the different epochs, though, have many features that differ significantly. When a mild constraint is applied to suppress differences not required by the data, all these artificial temporal changes disappear (Figure 6).

Systematic Swarm-Like Variations in Ray Distribution

In reality, temporal changes in earthquake locations are often more systematic than those considered above. An extreme but important example is afforded by earthquake swarms and aftershock sequences, which often produce tens of thousands of arrival-time data densely sampling a volume that previously was sampled sparsely or not at all.

Figure 7 shows rays for 100 pseudo-random hypocenters intended to mimic an earthquake swarm. The hypocenters are distributed with uniform probability density throughout a 2 km × 2 km × 2 km cube located in the center of the region. This ray distribution is quite different from ones like that shown in Figure 4, and it samples the structure poorly. Inverting theoretical data from it produces models with significant structural features concentrated mainly near the region of seismic activity (Figure 8(b)). Such models differ greatly from ones obtained from inverting a more uniform (e.g. pre-swarm) seismicity distribution (Figure 8(a)) and such differences might well be mistaken for real temporal variations related to the earthquake-generation process. Another environment in which this effect could be important is "Enhanced Geothermal Systems" (EGS) hydrofracturing experiments, which induce spatially concentrated seismicity that could produce tomographic artifacts that could be mistaken for induced changes in rock properties.

Jointly inverting such an aftershock-like data set and one with uniformly distributed rays, however, eliminates the misleading apparent temporal change (Figure 9). The strong concentration of rays in the neighborhood of the aftershocks strongly biases the derived models (compare Figure 9 with Figure 6, for example), but does not produce spurious temporal variations in wave speed.

True Temporal Variations in Wave Speeds

To demonstrate that *tomo4d* not only suppresses artificial temporal variations in wave speed but also can reveal true temporal variations, we conducted tests using synthetic data for models that vary slightly between epochs. In order to pose a severe test, we used the strongly differing ray distributions shown in Figures 4 and 7, for the two epochs (as was done in the previous section). The structure for the first epoch is the same as the one used in all the previous examples, but for the second epoch we introduced a 0.1 km/s negative V_P anomaly in a 2 × 2 × 1 km region just below sea level in the northwestern part of the model.

Figure 10 shows the results of independent inversions. As in the case shown in Figure 5, the difference in the sampling of the structure provided by the two pseudo-random hypocenter distributions produces strong differences between the derived structures, and these completely obscure the temporal change in the northwest. Figure 11 shows the results of applying *tomo4d*. The results for the two epochs are now quite similar except in the shallow volume in the northwest, where the negative V_P anomaly that we introduced for the second epoch is clearly detectable. Because of the inevitably imperfect sampling of the structure by the rays, the anomaly is smeared vertically, and is visually detectable on Figure 11 from the surface to depths of about 2 km below sea level.

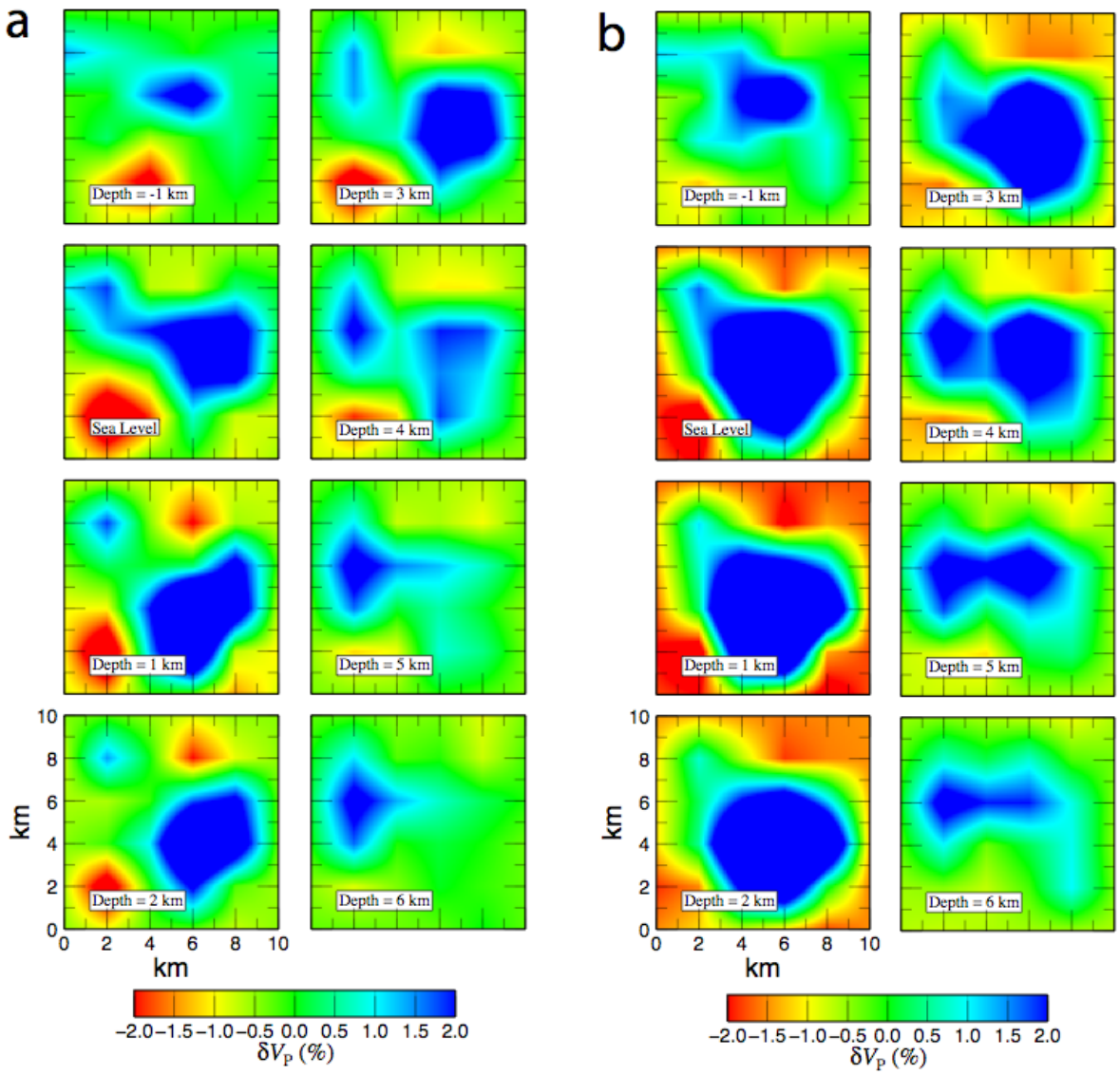

Fig. 5: *Maps for different depths showing the results (a and b) of independent inversions of a pair of theoretical arrival-time data sets intended to represent spatially uniform background seismicity. The data sets have a sparse statistically uniform seismicity distribution like that shown in Figure 4 (100 events and 1300 rays per data set). Because of different spatial sampling of the three-dimensional structure, the models exhibit differences that could be mistaken for temporal variations.*

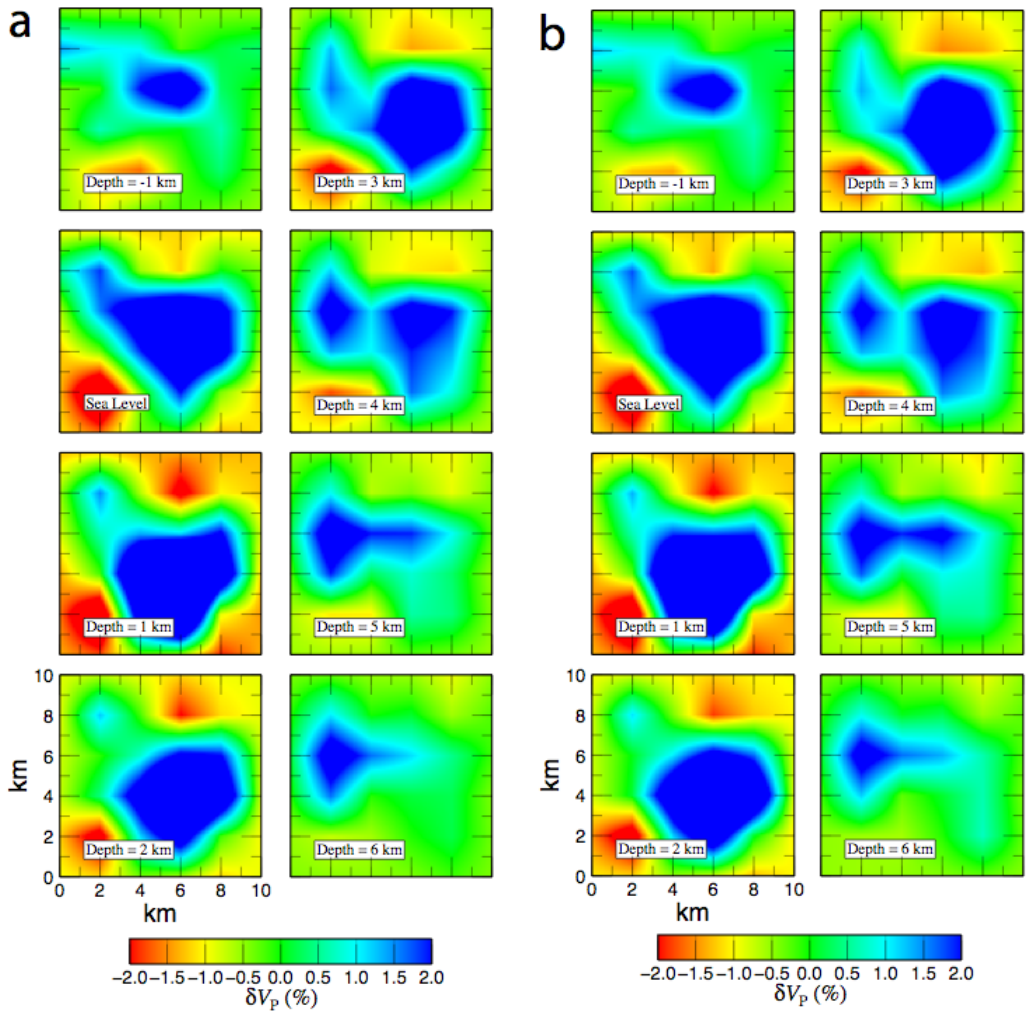

Fig. 6: *Maps like those of Figure 5 showing the results of inverting the same theoretical data sets, but imposing a weak constraint to minimize differences that are not truly required by the data. Artificial differences between the results for different epochs are practically eliminated.*

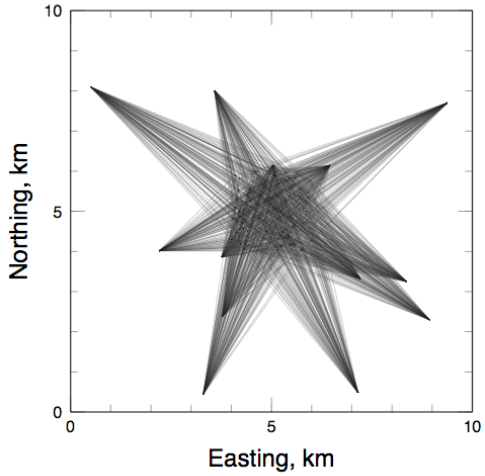

Fig. 7: *Surface projections of computed ray paths (represented as straight lines) for a pseudo-random theoretical arrival-time data set intended to represent data from an earthquake swarm or aftershock sequence. Rays connect each of 100 pseudo-random hypocenter locations, uniformly distributed in a 2 km × 2 km × 2 km cube centered at x = y = z = 5 km, to each seismometer.*

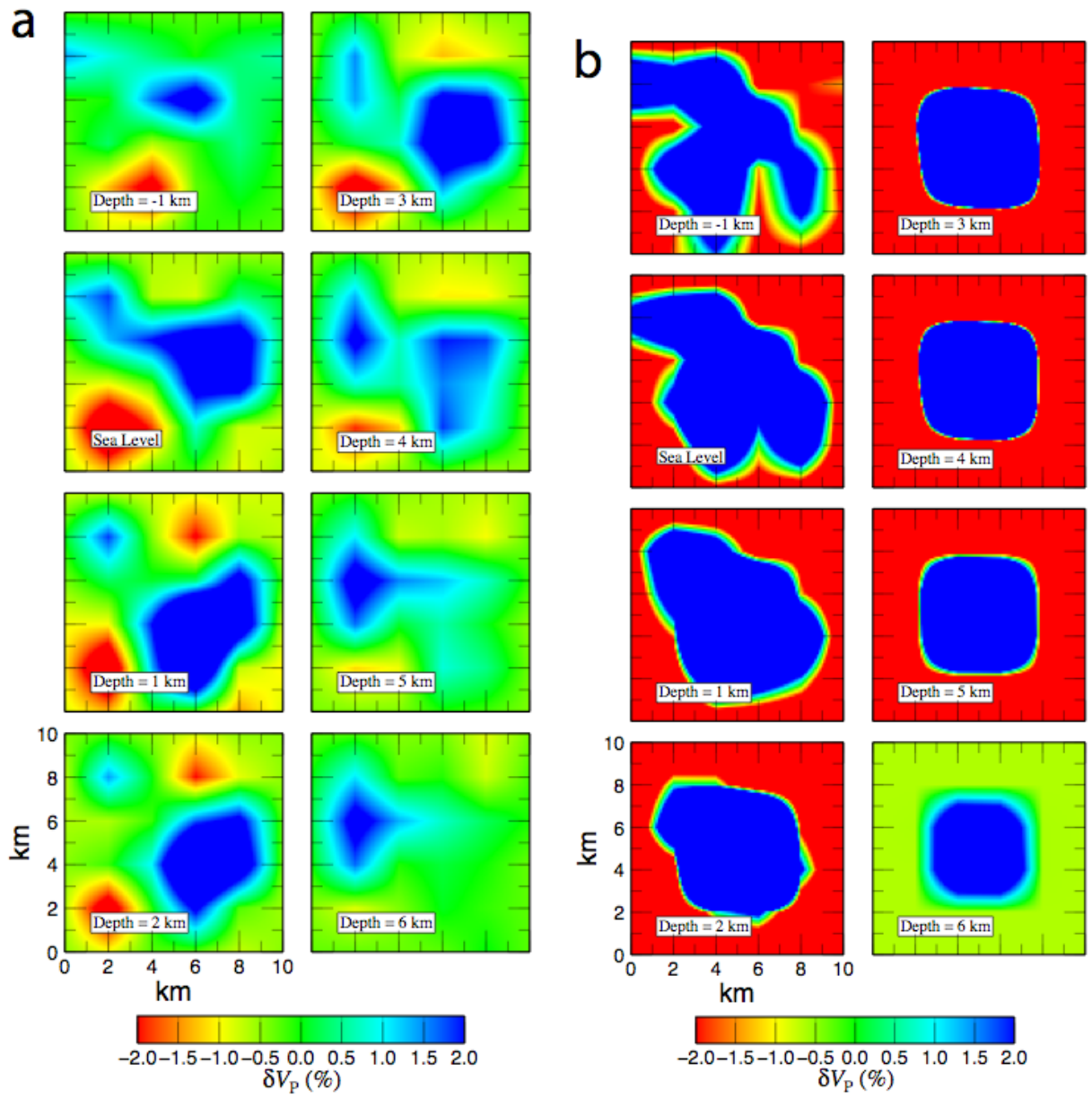

Fig. 8. *Maps for different depths showing the results of independent inversions of a pair of theoretical arrival-time data sets intended to represent the onset of an earthquake swarm or aftershock sequence. (a): The result derived from the earthquake distribution shown in Figure 4, representing pre-swarm background seismicity (identical to Figure 5a); (b): The result derived from the earthquake distribution shown in Figure 7, representing localized swarm seismicity. The systematic difference in the sampling of the structure by the two ray distributions produces strong differences in the results, especially in the seismically active volume. These differences could easily be mistaken for temporal variations in the wave speed.*

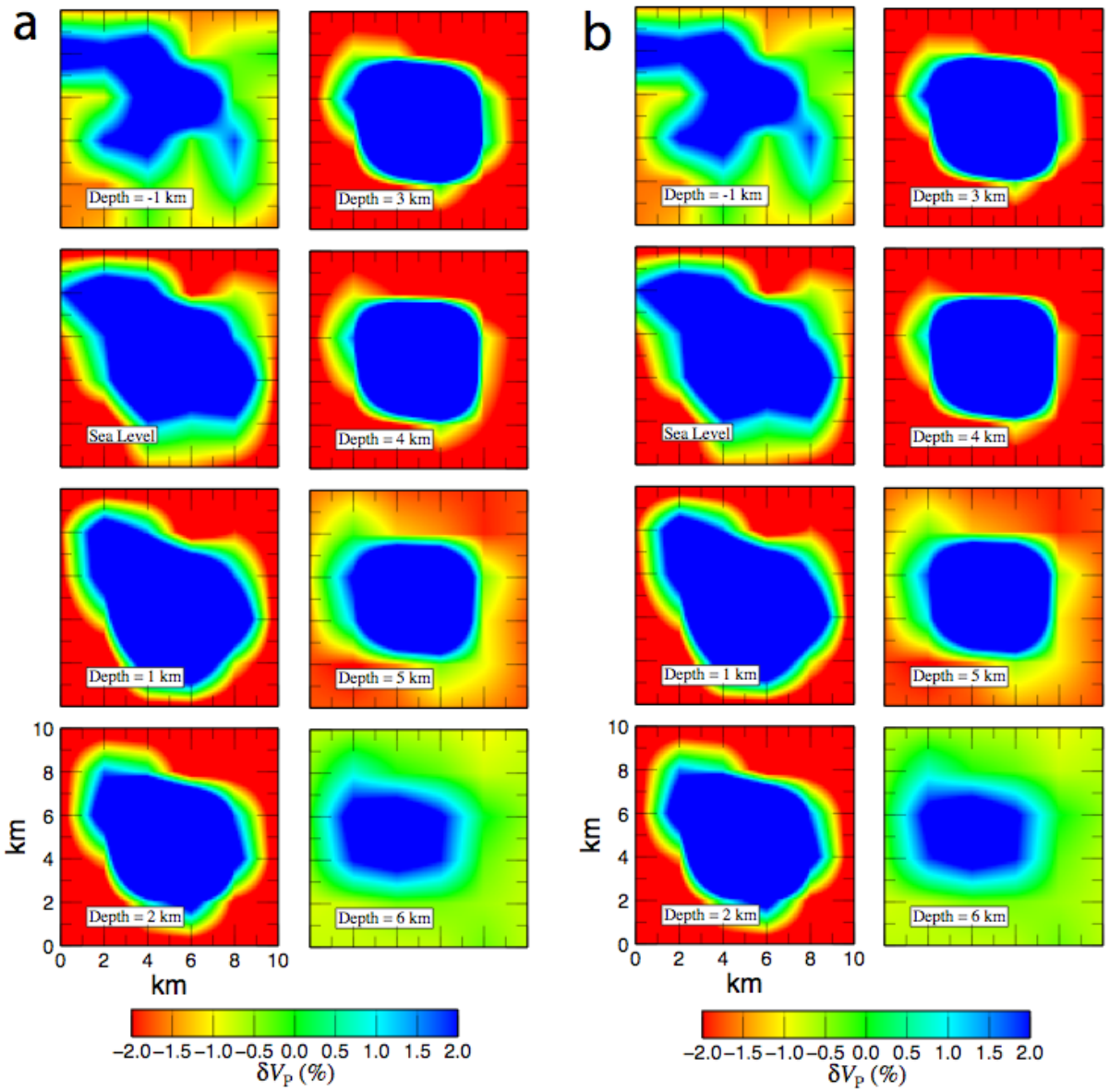

Fig. 9. *Maps like those of Figure 8 showing results obtained by inverting the same theoretical data sets, but imposing a weak constraint to minimize differences that are not truly required by the data. Because of the highly non-uniform ray distribution, the results differ significantly from ones such as those shown in Figure 6, but the spurious temporal variations that dominated Figure 8 have almost completely disappeared.*

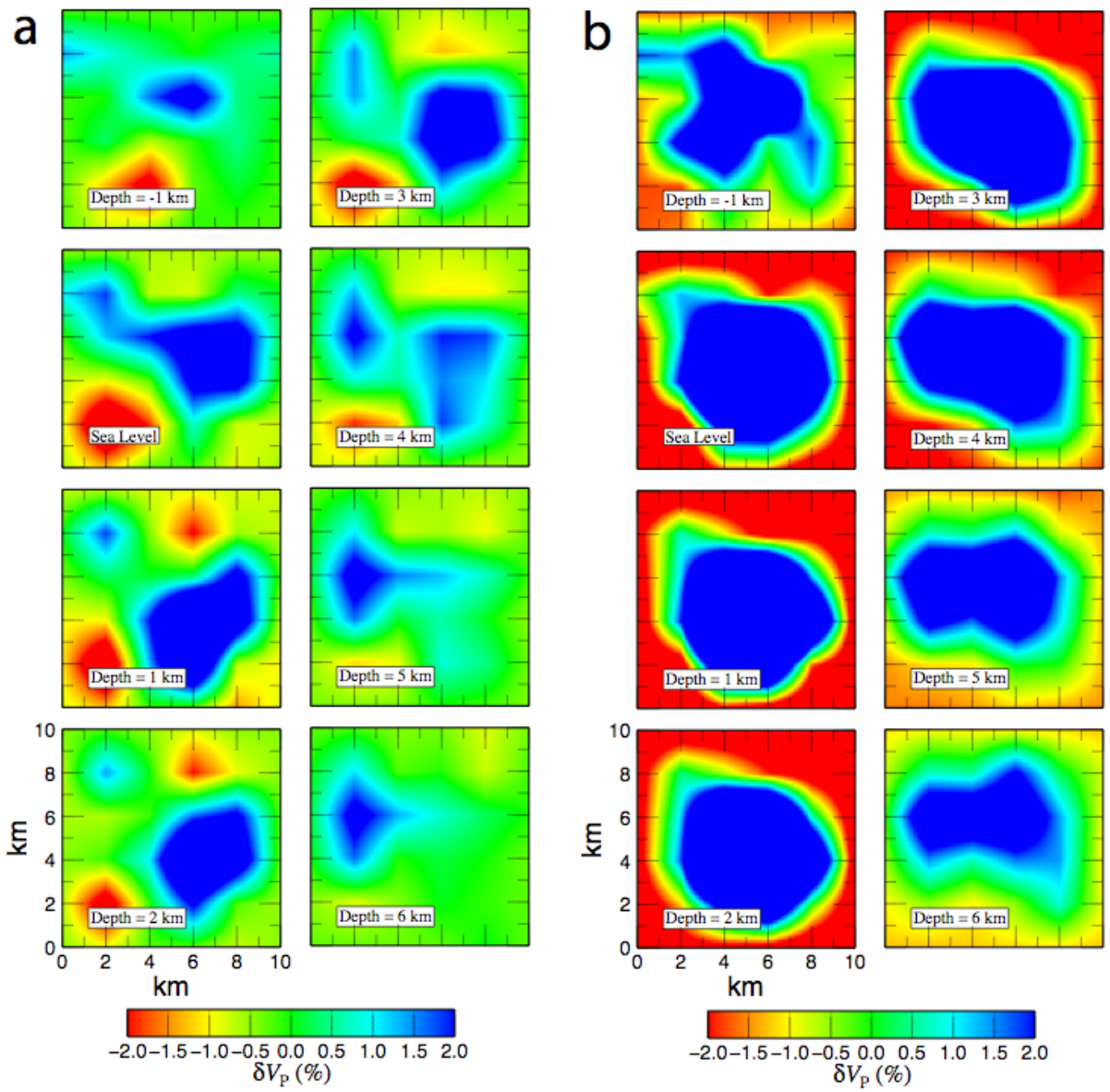

Fig. 10. Maps showing wave speeds obtained by independently inverting synthetic data sets computed for a weak, localized temporal change in wave speed. The model in (a) is derived from the same data set as that used for Figures 5(a) and 8(a). That in (b) is based on the same pseudo-random set of hypocenters as Figure 5(b) and a model with a −0.1 km/s V_P anomaly from sea level to 1 km below sea level, north coordinate from 6 to 8 km, and east coordinate from 2 to 4 km. The artificial temporal changes completely obscure all evidence of the true change.

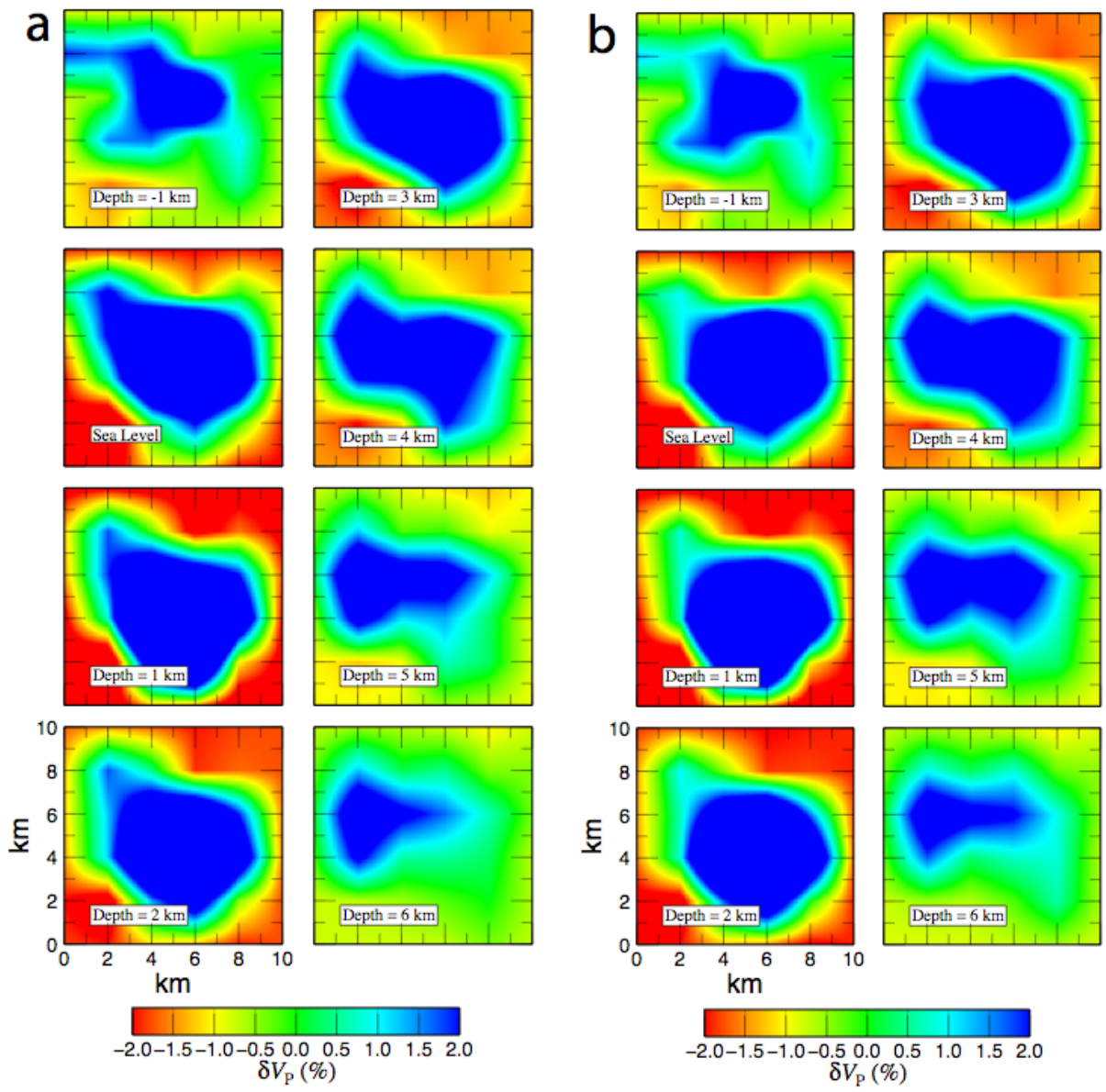

Fig. 11. Maps showing wave speeds in models obtained by inverting the same data sets as in Figure 10, but using tomo4d to suppress artificial apparent temporal changes. The change in wave speed near sea level in the northwest is now clear.

CONCLUSIONS

Repeat seismic tomography can detect and spatially resolve temporal changes in the seismic-wave speeds in the Earth, but it is subject to bias caused by temporal variations in ray paths caused by changes in earthquake locations or seismometer-network geometry, and also by random observational errors in measured arrival times. These effects can produce spurious and potentially misleading apparent temporal changes in derived tomographic models. Bias of this kind can be eliminated by inverting data sets from multiple epochs simultaneously, imposing constraints to minimize inter-epoch differences between models. Direct application of this method requires solution of a large system of linear equations, which is expensive in terms of both storage requirements and numerical labor. The particular structure of the equations, however, and their sparse-ness, make it possible to simultaneously invert data from two epochs with about twice the storage and twice the numerical effort as inverting a single data set. The algorithm for doing this is equally applicable to any linear or linearized inverse

problem, such as gravity, electrical, or magnetotelluric interpretation, in addition to seismic tomography.

REFERENCES

Boitnott, G.N. & Boyd, P.J. (1996), "Permeability, electrical impedance, and acoustic velocities of reservoir rocks from The Geysers geothermal field", in Twenty-first Workshop on Geothermal Reservoir Engineering, Stanford, California, Stanford University, 343-350.

Daley, T.M., Solbau, R.D., Ajo-Franklin, J.B., and Benson, S.M. (2007), "Continuous active-source seismic monitoring of CO_2 injection in a brine aquifer", *Geophysics*, **72**, A57-A61.

Foulger, G.R., Julian, B.R., Pitt, A.M., Hill, D.P., Malin, P.E. & Shalev, E. (2003), "Three-dimensional crustal structure of Long Valley caldera, California, and evidence for the migration of CO_2 under Mammoth Mountain", *J. geophys. Res.*, **108**, 2147, doi:2110.1029/2000JB000041.

Gunasekera, R.C., Foulger, G.R. and Julian, B.R. (2003), Reservoir depletion at The Geysers geothermal area, California, shown by four-dimensional seismic tomography. *J. Geophys. Res.*, 108(B3), 2134,doi:10.1029/2001JB000638.

Julian, B.R., and Foulger, G.R. (2009), "Time-dependent seismic tomography", in preparation.

Julian, B.R., G.R. Foulger and F. Monastero, Time-dependent seismic tomography and its application to the Coso geothermal area, 1996-2006, Proceedings, *Thirty-Third Workshop on Geothermal Reservoir Engineering, Stanford University, Stanford, California*, January 28-30, SGP-TR-185, 387-390, 2008.

Marquardt, D.W. (1963), "An algorithm for least-squares estimation of nonlinear parameters", *J. SIAM*, **11**, 431-441.

Wang, Z., Cates, M.E., and Langan, R.T. (1998), "Seismic monitoring of a CO_2 flood in a carbonate reservoir: A rock physics study", *Geophysics*, **63**, 1604-1617.